

UPLINK PERFORMANCE OF MASSIVE MIMO SUBJECT TO DELAYED CSIT AND ANTICIPATED CHANNEL PREDICTION

Anastasios K. Papazafeiropoulos and Tharmalingam Ratnarajah

Institute for Digital Communications (IDCoM)
University of Edinburgh, EH9 3JL Edinburgh, UK
Email: {A.Papazaf, T.Ratnarajah}@ed.ac.uk

ABSTRACT

We consider a realistic cellular multi-user uplink channel with an excess of base station (BS) antennas, where the number of BS antennas and the number of users per cell increase at the same rate. Specifically, we investigate the negative impact of delayed channel state information at the transmitter (CSIT), when a minimum-mean-square-error (MMSE) detector is applied. Nevertheless, channel prediction is used for overcoming delayed CSIT degradation. We provide the asymptotic signal-to-interference-plus-noise ratios (SINRs) that demonstrate not only their dependence on delayed and predicted CSIT, but also the outperformance of MMSE against maximal ratio combiner (MRC). The deterministic nature of the results renders them easily computed, while simulations show their accuracy even for practical system dimensions.

1. INTRODUCTION

Massive multiple-input multiple-output (MIMO) system is currently considered as an effective and promising solution for achieving high data rates in cellular networks [1–4]. In particular, increasing the number of base station (BS) antennas M achieves higher capacity. In addition, multi-user processing is simplified, since the effects of fast fading, intra-cell interference, and thermal noise vanish [1]. Nevertheless, high energy efficiency is achieved, if the transmit power is reduced by $O(\sqrt{M})$, while maintaining a fixed per user information rate [3].

In the burgeoning literature on massive MIMO, linear detectors have attracted a lot of attention due to their optimal behavior as the of BS antennas goes to infinity [1]. Remarkably, deterministic approximations of the uplink signal-to-interference-plus-noise ratios (SINRs) with maximal ratio combiner (MRC) and minimum mean-square error (MMSE) receivers proved to be tight even for moderate number of BS antennas and users [4]. Taking into account that channel state information at the transmitter (CSIT) in real systems is imperfect, an effort was made for characterizing the degradation of the uplink SINR with MRC due to the relative movement between the antennas and the scatterers in [5]. Basically, this effect causes a temporal variation of the CSI, which is acquired with a finite delay at the transmitter.

In this work, we cover the arising need for further study of the uplink channel of massive MIMO systems with delayed CSIT by applying a MMSE decoder. Specifically, we derive the deterministic equivalent sum rate with MMSE accounting for delayed CSIT.

This research was supported by a Marie Curie Intra European Fellowship and HARP project within the 7th European Community Framework Programme for Research of the European Commission under grant agreements no. [330806], IAWICOM and no. [318489], HARP.

Notably, the sum rate becomes negligible for certain Doppler shifts. Moreover, use of the technique, developed in [5], enables us to obtain the deterministic uplink sum rate that accounts for predicted CSIT by means of a Wiener filter. Finally, comparison of the proposed results with those in [5] shows the outperformance of MMSE against MRC. Note the valuable contribution of the results due to their deterministic nature and their accuracy even for realistic system dimensions, which allow for further optimization without the need of lengthy simulations.

2. SYSTEM MODEL

We consider the uplink of a multicell system with L BSs, having N antennas each, and K single antenna users per cell transmitting simultaneously. Hereafter, the index r denotes the uplink (reverse) channel. The baseband signal $\mathbf{y}_{r,j} \in \mathbb{C}^N$ received at BS j at time instant n is given as

$$\mathbf{y}_{r,j}[n] = \sqrt{p_r} \sum_{l=1}^L \mathbf{H}_{jl} \mathbf{x}_{r,l}[n] + \mathbf{z}_{r,j}[n], \quad (1)$$

where $p_r > 0$ denotes the average transmit signal-to-noise ratio (SNR), $\mathbf{H}_{jl} = [\mathbf{h}_{jl1}[n], \mathbf{h}_{jl2}[n], \dots, \mathbf{h}_{jlK}[n]] \in \mathbb{C}^{N \times K}$ is the channel matrix from the users in cell l to BS j , $\mathbf{x}_{r,l} = [x_{r,l1}, \dots, x_{r,lK}]^T \sim \mathcal{CN}(\mathbf{0}, \mathbf{I}_K)$ is the transmit symbol vector from the users in cell l with mutually independent elements, and $\mathbf{z}_{r,j} \sim \mathcal{CN}(\mathbf{0}, \sigma_j^2 \mathbf{I}_N)$ is the noise vector.

The channel vector \mathbf{h}_{jlk} at time slot $[n]$ is modelled as

$$\mathbf{h}_{jlk}[n] = \mathbf{R}_{jlk}^{1/2} \mathbf{g}_{jlk}[n], \quad (2)$$

where $\mathbf{R}_{jlk} \in \mathbb{C}^{N \times N}$ is a deterministic Hermitian-symmetric positive definite matrix capable of describing various effects (e.g. path loss and spatial correlation due to limited antenna spacing). Fast fading is described by means of the uncorrelated Gaussian channel vector $\mathbf{g}_{jlk}[n] \in \mathbb{C}^N$ having zero mean and unit variance, i.e. $\mathbf{g}_{jlk}[n] \sim \mathcal{CN}(\mathbf{0}, \mathbf{I}_N)$.

3. CHANNEL IMPAIRMENTS AND PREDICTION

Multi-user channels promise high multiplexing gains, if perfect current CSIT is known. Unfortunately, this is inevitable in real channels. Towards a more realistic analysis, we consider the well studied pilot contamination and the delayed CSIT due to time variation of the channel. Moreover, we achieve prediction of the current state by means of a Wiener filter.

3.1. Pilot Contamination

In the uplink training phase, the user terminals send sequences (pilots) that allow the base stations estimate their local channel $\hat{\mathbf{H}}_{jj}$. The interference coming from users using the same sequence but belonging to other cells is known as pilot contamination. This effect necessitates the use of MMSE as

$$\mathbf{h}_{jlm}[n] = \hat{\mathbf{h}}_{jlm}[n] + \tilde{\mathbf{h}}_{jlm}[n], \quad (3)$$

where $\hat{\mathbf{h}}_{jlm}[n] \sim \mathcal{CN}(\mathbf{0}, \Phi_{jlm})$ is the the estimated channel and $\tilde{\mathbf{h}}_{jlm}[n] \sim \mathcal{CN}(\mathbf{0}, \mathbf{R}_{jlm} - \Phi_{jlm})$ is the channel estimation error with Φ_{jlm} defined in [4]. Note that $\hat{\mathbf{h}}_{jlm}[n]$ and $\tilde{\mathbf{h}}_{jlm}[n]$ are statistically independent because they are uncorrelated and jointly Gaussian, as well as $\mathbf{R}_{jlm}, \mathbf{Q}_{jm}$, and Φ_{jlm} are independent of $n \forall j, l$, and m .

3.2. Delayed CSIT

The transmitter obtains CSI indirectly by assuming channel reciprocity. However, this requires the forward and reverse links to occur at the same time. Unfortunately, a delay appears, which is inherent in real channels due to the channel time variation coming from the relative movement between the antennas and the scatterers. Nevertheless, without loss of generality, we assume that all users move with the same velocity. As a result, the time variation does not depend on the user index.

We relate the past samples of the fading channel with its current state by means of the application of the autoregressive model of order L [6]. Keeping complexity in logical levels without sacrificing enough accuracy allows to consider $L = 1$. Otherwise, the design of predictors would be prohibitive, since many parameters should be estimated. Thus, the current channel between the j th BS and the m th interfering user is

$$\mathbf{h}_{jlm}[n] = \alpha \mathbf{h}_{jlm}[n-1] + \mathbf{e}_{jlm}[n], \quad (4)$$

where $\mathbf{h}_{jlm}[n-1]$ is the channel in the previous symbol duration and $\mathbf{e}_{jlm}[n] \in \mathbb{C}^N$ is an uncorrelated channel error modelled as a stationary Gaussian random process with i.i.d. entries and distribution $\mathcal{CN}(\mathbf{0}, (1 - \alpha^2)\mathbf{R}_{jlm})$.

The time variation of the channel can be expressed by the widely accepted autocorrelation function of the Jakes model [7]

$$r_h[k] = J_0(2\pi f_D T_s |k|), \quad (5)$$

where $J_0(\cdot)$ is the zeroth-order Bessel function of the first kind, T_s is the channel sampling duration, $|k|$ is the delay in terms of the number of symbols, and $f_D = \frac{vf_c}{c}$ is the maximum Doppler shift (v is the velocity of the user in m/s , $c = 3 \times 10^8$ m/s is the speed of light, and f_c is the carrier frequency). In particular, we assign $\alpha = r_h[1]$ to denote the temporal variation.

Overall, we can incorporate both the effects of pilot contamination and delayed CSIT as

$$\mathbf{h}_{jjm}[n+1] \stackrel{(3)}{=} \alpha \hat{\mathbf{h}}_{jjm}[n] + \tilde{\mathbf{e}}_{jjm}[n+1], \quad (6)$$

where $\tilde{\mathbf{e}}_{jjm}[n+1] \sim \mathcal{CN}(\mathbf{0}, \mathbf{R}_{jjm} - \alpha^2 \Phi_{jjm})$ and $\hat{\mathbf{h}}_{jjm}[n]$ are mutually independent. As you can see, the combined error $\tilde{\mathbf{e}}_{jjm}[n+1]$ depends on both the pilot contamination and delayed CSIT effects, allowing the export of interesting outcomes during the following analysis.

3.3. Channel Prediction

Prediction of the current channel state from delayed measurements confronts the effect of delayed CSIT due to temporal variation. Thus, suppose that we apply the p -th order linear Wiener predictor $\mathbf{V}_{jjm} = [\mathbf{V}_{jjm,0} \ \mathbf{V}_{jjm,1} \ \cdots \ \mathbf{V}_{jjm,p}] \in \mathbb{C}^{N \times N(p+1)}$, obtained in [5] as

$$\mathbf{V}_{jjm} = \alpha [\delta(p, \alpha) \otimes \mathbf{R}_{jjm}] \mathbf{T}_{jm}(p, \alpha), \quad (7)$$

where we provide the following definitions

$$\begin{aligned} \delta(p, \alpha) &= [1 \ \alpha \ \cdots \ \alpha^p] \\ \Delta(p, \alpha) &= \begin{pmatrix} 1 & \alpha & \cdots & \alpha^p \\ \alpha & 1 & \cdots & \alpha^{p-1} \\ \vdots & \vdots & \ddots & \vdots \\ \alpha^p & \alpha^{p-1} & \cdots & 1 \end{pmatrix} \\ \mathbf{T}_{jm}(p, \alpha) &= \left[\Delta(p, \alpha) \otimes \sum_{l=1}^L \mathbf{R}_{jlm} + \frac{\sigma_b^2}{p\tau} \mathbf{I}_{N(p+1)} \right]^{-1} \\ \Theta_{jlm}(p, \alpha) &= [\delta(p, \alpha) \otimes \mathbf{R}_{jjm}] \mathbf{T}_{jm}(p, \alpha)^H [\delta(p, \alpha) \otimes \mathbf{R}_{jlm}]^H. \end{aligned}$$

This filter provides us the predicted channel

$$\bar{\mathbf{h}}_{jjm}[n+1] = \sum_{q=0}^p \mathbf{V}_{jjm,q} \bar{\mathbf{y}}_{p,jm}[n-q] = \mathbf{V}_{jjm} \bar{\mathbf{y}}_{p,jm}[n], \quad (8)$$

where $\bar{\mathbf{y}}_{p,bu}[n] = [\bar{\mathbf{y}}_{p,bu}^H[n] \ \cdots \ \bar{\mathbf{y}}_{p,bu}^H[n-p]]^H \in \mathbb{C}^{N(p+1) \times 1}$.

The current channel can be derived from its predicted version as

$$\mathbf{h}_{jjm}[n+1] = \bar{\mathbf{h}}_{jjm}[n+1] + \check{\mathbf{h}}_{jjm}[n+1], \quad (9)$$

where $\bar{\mathbf{h}}_{jjm}[n+1]$ and $\check{\mathbf{h}}_{jjm}[n+1]$ are uncorrelated with covariance matrices $\mathbf{R}_{jjm} - \alpha^2 \Theta_{jlm}(p, \alpha)$ and $\alpha^2 \Theta_{jlm}(p, \alpha)$, respectively. Note that the zeroth order filter provides $\bar{\mathbf{h}}_{jjm}[n+1] = \alpha \hat{\mathbf{h}}_{jjm}[n]$, i.e., no channel prediction as expected.

4. UPLINK ASYMPTOTIC ANALYSIS

This section presents our main technical results. All proofs are provided in [8] due to limited space. The theory of deterministic equivalents offers the derivation of asymptotic results as $K, N \rightarrow \infty$, while keeping a finite ratio K/N .

We consider that BS j has knowledge of CSI $\mathbf{g}_{jjm}[n+1]$, which differentiates among specific conditions. Thus, in case of knowledge of current CSI at time $n+1$, the channel is not perfect but estimated due to pilot contamination, i.e., $\mathbf{g}_{jjm}[n+1] = \hat{\mathbf{h}}_{jjm}[n+1]$. Similarly, the delayed and predicted CSI are given by $\mathbf{g}_{jjm}[n+1] = \alpha \hat{\mathbf{h}}_{jjm}[n]$ and $\mathbf{g}_{jjm}[n+1] = \bar{\mathbf{h}}_{jjm}[n+1]$, respectively.

The received signal after application of a linear detector $\mathbf{W}_j[n] \in \mathbb{C}^{N \times K}$ to $\mathbf{y}_{r,j}[n]$ is (scaled by $1/\sqrt{p_r}$)

$$\begin{aligned} \tilde{\mathbf{y}}_{r,jm}[n+1] &= \mathbf{w}_{jm}^H[n+1] \mathbf{g}_{jjm}[n+1] x_{r,jm}[n+1] \\ &+ \mathbf{w}_{jm}^H[n+1] (\mathbf{h}_{jjm}[n+1] - \mathbf{g}_{jjm}[n+1]) x_{r,jm}[n+1] \\ &+ \sum_{(l,k) \neq (j,m)} \mathbf{w}_{jm}^H[n+1] \mathbf{h}_{jlk}[n+1] x_{r,lk}[n+1] \\ &+ \frac{1}{\sqrt{p_r}} \tilde{\mathbf{z}}_{r,jm}[n+1], \end{aligned} \quad (10)$$

where $\tilde{\mathbf{z}}_{r,jm} = \mathbf{w}_{r,jm}^H[n] \mathbf{z}_{r,jm}[n]$ is spatially filtered Gaussian noise and $\mathbf{w}_{r,jm}^H[n]$ is the m th column of $\mathbf{W}_j[n]$. The temporal parameter

α and $\mathbf{R}_{jlm} \forall l$ are assumed known. $\tilde{y}_{r,jm}[n+1]$ can be described as the received signal of a single-input single-output (SISO) system with the effective channel to be $\mathbf{g}_{jjm}[n+1]$, while and any other term constituting uncorrelated additive Gaussian noise. Thus, the desired signal power is

$$S_{r,jm} = |\mathbf{w}_{jm}^H[n+1] \mathbf{g}_{jjm}[n+1]|^2, \quad (11)$$

while the term concerning the interference and noise powers is

$$I_{r,jm} = |\mathbf{w}_{jm}^H[n+1] (\mathbf{h}_{jjm}[n+1] - \mathbf{g}_{jjm}[n+1])|^2 + \frac{\sigma_j^2}{p_r} \left\| \mathbf{w}_{jm}^H[n+1] \right\|^2 + \sum_{(l,k) \neq (j,m)} |\mathbf{w}_{jm}^H[n+1] \mathbf{h}_{jlk}[n+1]|^2. \quad (12)$$

The linear filter, taken into account, is the MMSE detector

$$\mathbf{w}_{jm}^{\text{MMSE}}[n+1] = \mathbf{\Sigma}_j^{(G)}[n+1] \mathbf{g}_{jjm}[n+1], \quad (13)$$

where $\mathbf{\Sigma}_j^{(G)}[n+1] = (\mathbf{G}_{jj}[n+1] \mathbf{G}_{jj}^H[n+1] + \mathbf{Z}_{r,j} + N \varphi_{r,j} \mathbf{I}_N)^{-1}$. Note that the design parameters $\varphi_{r,j} > 0$ and $\mathbf{Z}_{r,j} \in \mathbb{C}^{N \times N}$, which is a Hermitian nonnegative definite matrix, can be optimized.

Theorems 1 and 2 present the deterministic equivalent uplink SINRs with MMSE detector that consider delayed and predicted CSI, respectively. Hence, our first result follows.

Theorem 1 *The deterministic equivalent uplink SINR for user m in cell j with MMSE detector, accounting for delayed CSI, is given by (14) with $\hat{\delta}_{jm} = \frac{1}{N} \text{tr} \mathbf{\Phi}_{jjm} \mathbf{T}_j$, $\hat{\delta}'_{r,jm} = \frac{1}{N} \text{tr} (\mathbf{R}_{jjm} - \alpha^2 \mathbf{\Phi}_{jjm}) \mathbf{T}_j^{r,d1}$, $\hat{\delta}''_{jm} = \frac{1}{N} \text{tr} \mathbf{\Phi}_{jjm} \mathbf{T}_j^{r,d2}$, $\hat{\vartheta}_{jlk} = \frac{1}{N} \text{tr} \mathbf{\Phi}_{jlk} \mathbf{T}_j$, $\hat{\vartheta}'_{jlk} = \frac{1}{N} \text{tr} \mathbf{\Phi}_{jlk} \mathbf{T}_j^{r,d1}$, and*

$$\hat{\mu}_{jlk} = \frac{\text{tr} \mathbf{R}_{jlk} \mathbf{T}_j^{r,d1}}{N} - \frac{2 \text{Re} \{ \hat{\vartheta}_{jlk}^* \hat{\vartheta}'_{jlk} \} (1 + \hat{\delta}_{jk}) - (\hat{\vartheta}_{jlk})^2 \hat{\delta}''_{jk}}{(1 + \hat{\delta}_{jk})^2},$$

where

- * $\mathbf{T}_j = \mathbf{T}(\phi_{r,j})$ and $\boldsymbol{\delta}_j = [\delta_{j1}, \dots, \delta_{jK}]^T = \boldsymbol{\delta}(\phi_{r,j})$ are given by [9, Theorem 1] for $\mathbf{D} = \mathbf{I}_N$, $\mathbf{S} = \mathbf{Z}_j/N$, $\mathbf{R}_k = \mathbf{\Phi}_{jjk} \forall k$,
- * $\mathbf{T}_j^{r,d1} = \mathbf{T}'(\phi_{r,j})$ is given by [4, Theorem 2] for $\mathbf{D} = \mathbf{I}_N$, $\mathbf{S} = \mathbf{Z}_j/N$, $\mathbf{K}^{r,d1} = \mathbf{\Phi}_{jjm}$, $\mathbf{R}_k = \mathbf{\Phi}_{jjk} \forall k$,
- * $\mathbf{T}_j^{r,d2} = \mathbf{T}'(\phi_{r,j})$ is given by [4, Theorem 2] for $\mathbf{D} = \mathbf{I}_N$, $\mathbf{S} = \mathbf{Z}_j/N$, $\mathbf{K}^{r,d2} = \mathbf{I}_N$, $\mathbf{R}_k = \mathbf{\Phi}_{jjk} \forall k$.

The second result corresponding to deterministic equivalent SINR for MMSE with predicted CSIT is:

Theorem 2 *The deterministic equivalent uplink SINR for user m in cell j with MMSE detector, accounting for predicted CSI by means of a p -th-order Wiener predictor, is given by (15) with $\bar{\delta}_{jm} = \frac{1}{N} \text{tr} \mathbf{\Theta}_{jjm}(p, \alpha) \mathbf{T}_j$, $\bar{\delta}'_{r,jm} = \frac{1}{N} \text{tr} (\mathbf{R}_{jjm} - \alpha^2 \mathbf{\Theta}_{jjm}(p, \alpha)) \mathbf{T}_j^{r,p1}$, $\bar{\delta}''_{jm} = \frac{1}{N} \text{tr} \mathbf{\Theta}_{jjm}(p, \alpha) \mathbf{T}_j^{r,p2}$, $\bar{\vartheta}_{jlk} = \frac{1}{N} \text{tr} \mathbf{\Theta}_{jlk}(p, \alpha) \mathbf{T}_j^{r,p2}$, $\bar{\vartheta}'_{jlk} = \frac{1}{N} \text{tr} \mathbf{\Theta}_{jlk}(p, \alpha) \mathbf{T}_j^{r,p1}$, and*

$$\bar{\mu}_{jlk} = \frac{\text{tr} \mathbf{R}_{jlk} \mathbf{T}_j^{r,p1}}{N} - \frac{2 \text{Re} \{ \alpha^4 \bar{\vartheta}_{jlk}^* \bar{\vartheta}'_{jlk} \} (1 + \alpha^2 \bar{\delta}_{jk}) - \alpha^6 (\bar{\vartheta}_{jlk})^2 \bar{\delta}''_{jk}}{(1 + \alpha^2 \bar{\delta}_{jk})^2},$$

where

- * $\mathbf{T}_j = \mathbf{T}(\phi_{r,j})$ and $\boldsymbol{\delta}_j = [\delta_{j1}, \dots, \delta_{jK}]^T = \boldsymbol{\delta}(\phi_{r,j})$ are given by [9, Theorem 1] for $\mathbf{D} = \mathbf{I}_N$, $\mathbf{S} = \mathbf{Z}_j/N$, $\mathbf{R}_k = \mathbf{\Phi}_{jjk} \forall k$,
- * $\mathbf{T}_j^{r,p1} = \mathbf{T}'(\phi_{r,j})$ is given by [4, Theorem 2] for $\mathbf{D} = \mathbf{I}_N$, $\mathbf{S} = \mathbf{Z}_j/N$, $\mathbf{K}^{r,p1} = \mathbf{\Theta}_{jjm}(p, \alpha)$, $\mathbf{R}_k = \mathbf{\Phi}_{jjk} \forall k$,
- * $\mathbf{T}_j^{r,p2} = \mathbf{T}'(\phi_{r,j})$ is given by [4, Theorem 2] for $\mathbf{D} = \mathbf{I}_N$, $\mathbf{S} = \mathbf{Z}_j/N$, $\mathbf{K}^{r,p2} = \mathbf{I}_N$, $\mathbf{R}_k = \mathbf{\Phi}_{jjk} \forall k$.

5. NUMERICAL RESULTS

In this section, we verify our analysis and demonstrate the outperformance of MMSE decoder under the effects of delayed CSI and pilot contamination, as well as its benefits over channel prediction in massive MIMO cellular networks. We assume a multi-cell network with $L = 5$ cells sharing the same frequency band. Each cell has normalized radius to one, while $K = 4$ users are uniformly distributed around each BS on a circle of radius 0.7. The physical model includes a distance-based path loss model, given by $\tilde{\mathbf{R}}_{jlk} = d_{jlk}^{-\beta} \mathbf{I}_N$, where d_{jlk} denotes the distance between BS j and user k in cell j with $\beta = 3.5$. Moreover, the transmit and training SNRs are $p_r = 8\text{dB}$ and $p_p = 5\text{dB}$, respectively. The design parameters for MMSE are $\varphi_{r,j} = \frac{1}{p_r}$ and $\mathbf{Z}_{r,j} = 0$. Monte-Carlo simulations of (6) and (9) provide the simulation curves for delayed and predicted CSIT, respectively. The analytical curves for MMSE as well as MRC are computed via (14), (15) as well as [5, eq. 53, 75], respectively. The simulated and analytical results match exactly, even for moderate values of N .

Figure 1 depicts the uplink sum rate of the users in the center cell as a function of the normalized Doppler shifts $f_D T_s$ for $N = 30, 60, 80$. Delayed CSIT decreases the uplink sum rate to zero with some ripples following according to the behaviour of the Bessel function $J_0(\cdot)$. Specifically, at $f_D T_s \approx 0.4$ we observe the first zero point and then with following ripples, the magnitude increases and later decreases to zero again and again, tending finally to zero. Note that increasing the number of BS antennas N induces higher sum rate, but the shape of the curves is kept the same by keeping the zero points at constant specific values of $f_D T_s$. Apparently, the dependence of MMSE by delayed CSIT is identical to MRC, although MMSE achieves higher sum rate under the same conditions, i.e., specific Doppler shift.

Fig. 2 illustrates the cumulative distribution function of the uplink deterministic equivalent sum rate of the users for different Doppler shifts, when $N = 90$. Also, the case of current CSIT with MMSE is shown as a benchmark. As expected, lower Doppler shift allows the transmission with a higher sum rate at a given probability. Specifically, MMSE achieves 19.18 b/s/Hz with $f_D T_s = 0.1$ and 15.14 b/s/Hz with $f_D T_s = 0.2$ against MRC, which achieves 16.95 b/s/Hz and 13.21 b/s/Hz, respectively.

The uplink sum rate of the users versus $f_D T_s$ for varying filter order p , as well as the sum rate with current CSIT are shown in Fig 3 ($N = 90$). Especially, in larger Doppler shifts, the ability of the filter to compensate for the loss because of the delayed CSIT weakens. Channel prediction with higher value of p , i.e., more observations in the past, is required, in order to predict with higher precision the degraded channel. Notably, MMSE behaves better by approaching closer than MRC the nominal value representing no delayed CSIT, i.e., current CSIT, as the Doppler shift increases.

$$\bar{\gamma}_{r,jm}(\alpha) = \frac{\alpha^2 \hat{\delta}_{jm}^2}{\frac{1}{N} \hat{\delta}'_{r,jm} + \frac{\sigma_j^2}{p_r} \frac{1}{N} \hat{\delta}''_{jm} + \sum_{(l,k) \neq (j,m)} \frac{1}{N} \hat{\mu}_{jlk m} + \alpha^2 \sum_{l \neq j} |\hat{\vartheta}_{jlm}|^2} \quad (14)$$

$$\bar{\gamma}_{r,jm}(\alpha) = \frac{\alpha^2 \bar{\delta}_{jm}^2}{\frac{1}{N} \bar{\delta}'_{r,jm} + \frac{\sigma_j^2}{p_r} \frac{1}{N} \bar{\delta}''_{jm} + \sum_{(l,k) \neq (j,m)} \frac{1}{N} \bar{\mu}_{jlk m} + \sum_{l \neq j} \alpha^{2(p+2)} |\bar{\vartheta}_{jlm}|^2} \quad (15)$$

6. CONCLUSION

We have studied the uplink performance of MMSE in a cellular multi-user MIMO system with the number of users and BS antennas getting large. In particular, we have derived approximations of achievable sum rates that account for delayed and predicted CSIT. Simulated results showed that the deterministic analytical results are reliable even for practical values of BS antennas N and users K . Most importantly, numerical results revealed that the sum rate becomes negligible for specific Doppler shifts. Nevertheless, we illustrate that MMSE appears a similar behaviour with MRC, although the former provides higher achievable sum rate and greater ability to predict the channel without sacrificing any complexity.

7. REFERENCES

- [1] T. L. Marzetta, "Noncooperative cellular wireless with unlimited numbers of base station antennas," *IEEE Trans. Wireless Commun.*, vol. 9, no. 11, pp. 3590–3600, Nov. 2010.
- [2] F. Rusek, D. Persson, B. K. Lau, E. G. Larsson, T. L. Marzetta, O. Edfors, and F. Tufvesson, "Scaling up MIMO: Opportunities and challenges with very large arrays," *IEEE Signal Process. Mag.*, vol. 30, no. 1, pp. 40–60, Aug. 2013.
- [3] H. Q. Ngo, E. G. Larsson, and T. L. Marzetta, "Energy and spectral efficiency of very large multiuser MIMO systems," *IEEE Trans. on Com.*, vol. 61, no. 4, pp. 1436–1449, Apr. 2013.
- [4] J. Hoydis, S. T. Brink, and M. Debbah, "Massive MIMO in the UL/DL of cellular networks: How many antennas do we need?," *IEEE J. Sel. Areas Commun.*, vol. 31, no. 2, pp. 160–171, Feb. 2013.
- [5] K. T. Truong and R. W. Heath, Jr., "Effects of Channel Aging in Massive MIMO Systems," *IEEE/KICS Journal of Communications and Networks, Special Issue on Massive MIMO*, vol. 15, no. 4, pp. 338–351, Aug. 2013, available on arXiv: 1305.6151.
- [6] K. E. Baddour and N. C. Beaulieu, "Autoregressive modelling for fading channel simulation," *IEEE Trans. Wireless Commun.*, vol. 4, no. 4, pp. 1650–1662, July 2005.
- [7] W. C. Jakes, *Microwave Mobile Communications*. New York: Wiley, 1974.
- [8] A. K. Papazafeiropoulos and T. Ratnarajah, "Performance Analysis of Massive MIMO Systems with Channel Impairments," 2013, submitted, available upon request.
- [9] S. Wagner, R. Couillet, M. Debbah, and D. T. M. Slock, "Large system analysis of linear precoding in correlated MISO broadcast channels under limited feedback," *IEEE Trans. Inf. Theory*, vol. 58, no. 7, pp. 4509–4537, Jul. 2012.

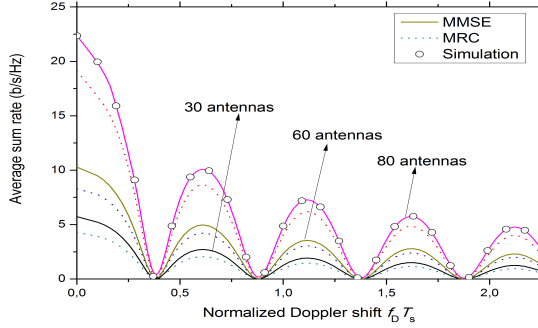


Fig. 1. Uplink sum rate versus the normalized Doppler shift $f_D T_s$ for different number of BS antennas N .

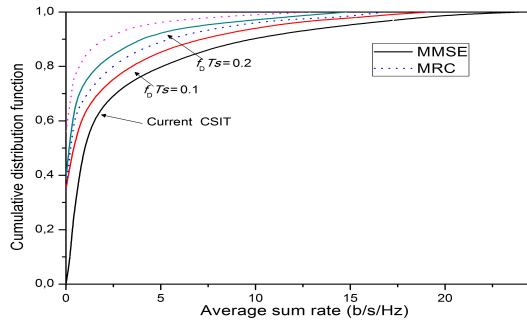


Fig. 2. The cumulative distribution function of the deterministic equivalent uplink sum rate for different normalized Doppler shifts $f_D T_s$.

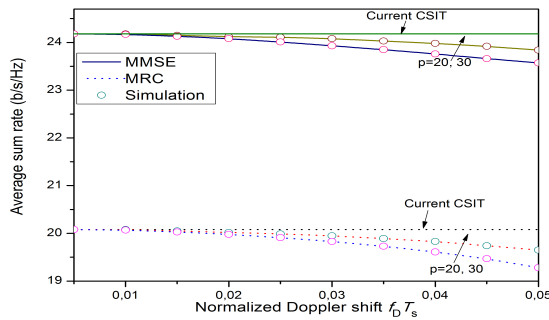


Fig. 3. Uplink sum rate versus the normalized Doppler shifts $f_D T_s$ for different order of the channel predictor.